Published in final edited form as:
Anal Chim Acta. 2009 October 5; 651(2): 201–208. doi:10.1016/j.aca.2009.08.032.

Isotopomer analysis of lipid biosynthesis by high resolution mass spectrometry and NMR

Andrew N. Lane[1,2], **Teresa W-M. Fan**[1,2,3], **Zhengzhi Xie**[2,3,4], **Hunter N.B. Moseley**[2,3], and **Richard M. Higashi**[2,3]

[1] JG Brown Cancer Center, 529 S. Jackson St., Louisville, KY 40202

[2] Center for Regulatory and Environmental Analytical Metabolomics (CREAM)

[3] Department of Chemistry, University of Louisville, Louisville, KY 40292

Abstract

We have coupled 2D-NMR and infusion FT-ICR-MS with computer-assisted assignment to profile ^{13}C-isotopologues of glycerophospholipids (GPL) directly in crude cell extracts, resulting in very high information throughput of >3000 isobaric molecules in a few minutes. A mass accuracy of better than 1 ppm combined with a resolution of 100,000 at the measured m/z was required to distinguish isotopomers from other GPL structures. Isotopologue analysis of GPLs extracted from LCC2 breast cancer cells grown on [U-^{13}C]-glucose provided a rich trove of information about the biosynthesis and turnover of the GPLs. The isotopologue intensity ratios from the FT-ICR-MS were accurate to ≈ 1% or better based on natural abundance background, and depended on the signal-to-nose ratio. The time course of incorporation of ^{13}C from [U-^{13}C]-glucose into a particular phosphatidylcholine was analyzed in detail, to provide a quantitative measure of the sizes of glycerol, acetyl CoA and total GPL pools in growing LCC2 cells. Independent and complementary analysis of the positional ^{13}C enrichment in the glycerol and fatty acyl chains obtained from high resolution 2D NMR was used to verify key aspects of the model. This technology enables simple and rapid sample preparation, has rapid analysis, and is generally applicable to unfractionated GPLs of almost any head group, and to mixtures of other classes of metabolites.

Keywords

stable isotopomer analysis; FT-ICR-MS; NMR; phospholipid biosynthesis

1. Introduction

The biosynthesis and turnover of lipids is an essential component of maintenance and growth of all cells, and they typically make up 10–20% of the cell dry weight [1]. In particular, dividing cells must double their lipid content on each passage through the cell cycle, and it is well-established that proliferating cancer cells up regulate expression or activity of both fatty acid synthase and acetyl CoA carboxylase, two key enzymes in fatty acid biosynthesis [2–5].

Correspondence to: A.N. Lane, JG Brown Cancer Center, 529 S. Jackson St., Louisville, KY 40202. anlane01@louisville.edu, Tel: 502 852 3067, Fax: 502 852 4311.
[4]Present address: Department of Medicine,

However, cells can also obtain fatty acids from the diet, and some unsaturated fatty acids are essential in mammals [6]. Errors in lipid metabolism have serious consequences for cellular integrity, and this has become a new area of research ("lipidomics") [7–10]. Thus cellular profiles of lipid turnover, and how they change in response to disease states or environmental insults is fundamental to our understanding of cellular disorders.

Although identification and quantification of the lipids present in a biological system is critical, it is equally important to determine their dynamic relationships, such as synthesis and turnover. This requires the use of tracer methods to follow atoms from source to product and to determine relative pool sizes of the precursors. Radiotracers have long been used for this purpose, but the detection methods generally provide little information about the number of positions actually labeled during biosynthesis [11,12]. Stable isotopes have also been used, [9,11,13,14], especially to measure lipid biosynthesis in cells or whole organisms, thus avoiding the use of hazardous radioisotopes [15–23].

Stable isotope tracing with MS and NMR detection has several advantages, including ease of handling, and the ability to measure a large number of labeled positions in a mixture of metabolites simultaneously. In particular, the ultra-high resolution and accurate mass capabilities of Fourier transform-ion cyclotron resonance-MS (FT-ICR-MS) can provide simultaneous determination of hundreds to thousands of lipid isotopologue and isotopomer species without chromatographic separation. This is a logical extension of current applications of MS [24–27] [28,29] [30] [31] and NMR [32] [33–35] on lipid profiling. By coupling with the many choices of stable isotope-enriched precursors (e.g. ^{13}C or ^{2}H-glucose or fatty acids labeled at different positions), detailed transformation pathways for a variety of lipids may be traced. Such information may lead to improved mechanistic understanding of lipid metabolism and how it is dysregulated in cellular disorders. However, to the best of our knowledge, systematic application of 2D NMR-based ^{13}C positional isotopomer with high mass resolution FT-ICR-MS isotopologue distributions to GPL mixtures, and the required instrument performances, have not been explored to date.

Over the last two decades, we have been using stable isotope tracer methods to follow metabolic transformations of ^{13}C and ^{15}N-labeled precursors into a variety of metabolites directly in crude extracts using MS and NMR detection without the need to use chromatographic separation [36–44]. Here we describe a ^{13}C mass spectrometry isotopologue-based analytical approach to measuring the net synthesis of GPLs in dividing breast cancer cells grown on [U-^{13}C]-glucose. Isotopologue distributions were determined as a function of labeling time using direct infusion nanospray FT-ICR-MS directly on crude extracts, without chromatographic separation, derivatization, or other chemical procedures. This analysis was enabled by exploiting the ultra high mass resolution that can differentiate neutrons from protons in intact, whole molecular species [30,46,47]. As [U-^{13}C]-glucose produces [U-$^{13}C3$]-glycerol and $^{13}C2$-acetyl CoA, the incorporation of these labeled precursors into GPLs adds 3 and 2n mass units to newly synthesized GPLs, which are readily distinguishable in the mass isotopologue profile. The FT-ICR-MS analysis was complemented by high-resolution 2D ^{1}H NMR that provides independent quantitative positional isotope distributions [36,38,40] of the glycerol and fatty acid moieties of the GPLs. This approach makes it possible to identify the isotopologues by inspection and straightforward integration of peaks provides the desired enrichments [40]. This combination of techniques provided both unambiguous assignment of GPL species, and a robust estimate of precursor pool sizes.

2. Experimental

2.1 Materials

[U-^{13}C]-glucose (99 atom%) was purchased from Sigma Aldrich (St. Louis, MO). RPMI 1640 medium and trypsin were purchased from Hyclone (Thermo Fisher Scientific, Waltham, MA), Biowest fetal bovine serum (FBS) from USA Scientific (Ocala, FL), and penicillin/ streptomycin from Atlanta Biologicals (Lawrenceville, GA).

Pure PC standards (DMPC, DPPC, DSPC and DOPC were obtained from Avanti Lipids (Alabaster, AL) to verify identification and isotope ratios at natural abundance. CD_3OD (>99.9 atom %) was purchased from Cambridge Isotope Laboratories, MA. Other solvents were of the highest reagent grade available.

2.2 Methods

2.2.1 Cell Culture and Treatment—The MCF7-LCC2 cell line was a generous gift of Dr. Young-Mee Park (Roswell Park Cancer Institute). Cells were cultured in RPMI medium containing 10% fetal bovine serum, 100 U/ml penicillin and 100 μg/ml streptomycin, 2 mM glutamine, and 0.2% unlabeled or uniformly labeled ^{13}C-glucose ([U-^{13}C]-Glc, at 37°C in a humidified growth chamber with 5% CO_2 atmosphere. Cells were grown for 3, 6, 11, and 24 hr before they were detached by 0.25% trypsin treatment, washed twice in excess ice-cold PBS, and spun at 1,700 g for 5 min at 4°C to obtain firm cell pellets. After removing PBS, cell pellets were immediately flash-frozen in liquid nitrogen and lyophilized.

GPLs were extracted using 100% methanol plus 1 mM butylated hydroxytoluene (BHT) as antioxidant in a ball mill (MM200, Retsch, Newtown, PA) with 3 mm diameter glass beads for 1 min. The methanolic extract was vacuum-dried in a Speedvac (Eppendorf, Westbury, NY), redissolved in 0.5 ml methanol plus 1 mM BHT, and filtered through a 0.45 μm regenerated cellulose membrane spin filter (Alltech Associates, Deerfield, IL). The filtrate was diluted 100 fold with 1.65 pmol/μL reserpine as an internal standard, 1mM BHT, plus 7.5 mM ammonium acetate in methanol, and then loaded onto 96-well microtiter plates for FT-ICR MS analysis. The undiluted extracts were used for NMR analysis (see below).

2.2.2 Mass spectrometry—Samples were analyzed on a hybrid linear ion trap - FT-ICR mass spectrometer (Finnigan LTQ FT, Thermo Electron, Bremen, Germany) equipped with a TriVersa NanoMate ion source (Advion BioSciences, Ithaca, NY) with an “A” electrospray chip (nozzle inner diameter 5.5 μm). The TriVersa NanoMate was operated in positive ion mode by applying 2.0 kV with no head pressure. MS runs were recorded over a mass range from 150 to 1300 Da. Initially, low resolution MS scans were acquired for 1 min to ensure the stability of ionization, after which high mass accuracy data were collected using the FT-ICR analyzer where MS scans were acquired for 8.5 min and at the target mass resolution of 100,000 at 800 m/z. The AGC (automatic gain control) maximum ion time was set to 500 ms (but typically utilized <10 ms) and five “μscans” were acquired for each saved spectrum; thus the cycle time for each transformed and saved spectrum was about 10 s. The LTQ-FT was tuned and calibrated according to the manufacturer’s default standard recommendations, which achieved better than 1ppm mass accuracy and capable of 400,000 resolution at m/z = 400.

FT-ICR mass spectra were exported as exact mass lists into an a spreadsheet file using QualBrowser 2.0 (Thermo Electron), typically exporting all of the observed peaks. Glycerophospholipid species were assigned based on their accurate mass [30], by first applying a small (typically <0.0005) linear correction based on the observed mass of the internal standard (reserpine), then using an in-house software tool PREMISE (PRecaculated Exact Mass Isotopologue Search Engine) (R.M. Higashi, unpublished) which was manually validated.

PREMISE is a straightforward routine that simply matches observed with theoretical m/z values, subject to a selectable window that was 0.0008 Da or smaller. For GPLs, the exact masses of a large number (>7000) of possible GPLs and their adducts (principally H and Na) are pre-calculated into a spreadsheet lookup table. In other words, PREMISE simply automates manual labor thousands of times per spectrum. The overall method is sufficient to assign a GPL to a particular class, i.e. total acyl chain length and degree of saturation, and headgroup identity.

2.2.3 NMR Analysis of GPL—Methanolic extracts of cells were freeze dried and redissolved in 100% d_4-methanol and loaded into 5 mm methanol susceptibility-matched Shigemi tubes (Shigemi Inc, Allison Park, PA). NMR spectra were recorded at 18.8 T on a Varian Inova spectrometer at 20°C. 1D ^{1}H and 1D ^{13}C HSQC spectra were recorded with a recycle time of 5 s. 2D TOCSY spectra were recorded with acquisition times of 0.3 s in t_2 and 0.042 s in t_1 using a 50 ms MLEV-17 spin-lock at a field strength of 9 kHz and a recycle time of 2 s. TOCSY data matrices were zerofilled once in t_2 to 8192 complex points and linear predicted and zero filled to 4096 complex points in t_1. Free induction decays were apodized using an unshifted Gaussian function and a 1-Hz line broadening exponential in both dimensions. Chemical shifts were referenced to the residual solvent methanol proton resonance at 3.32 ppm. Final spectra were baseline corrected and carefully phased for integration. Peak volumes were integrated using the Varian VNMR software and corrected for differential relaxation as previously described [38,40]. Where possible, 2D integrations were compared with 1D integrations, which showed that the accuracy of the enrichment was within ±2%. This is comparable to the analytical precision of the method for the technique. DMPC, DPPC, DSPC and DOPC standards were recorded under identical conditions for assignment of resonances, and to measure accurate T_1 values of protons attached to ^{12}C and ^{13}C (satellites) using inversion recovery.

2.3 Model Description

The carbon-skeleton of a GPL such as phosphatidylcholine (PC) comprises a 5-carbon phosphocholine unit attached to a three carbon glycerol backbone that is esterified to two fatty acyl chains at the 1 and 2 positions (Figure 1). In mammalian cells, the choline moiety derives from the medium, whereas the glycerol phosphate and fatty acids can be synthesized *de novo*, be obtained from the medium or by recycling existing membranes or internal stores of triglycerides. In dividing cells, there is a net synthesis of GPLs, and glucose is a major source of the carbon. Biosynthetically, glycerol phosphate derives from dihydroxyacetone-3-phosphate (DHAP), a glycolytic intermediate. The fatty acids are built up from acetyl CoA, which can be made from pyruvate deriving from numerous sources including glucose. Thus, there are 5 components or precursors, namely glycerol phosphate, acetyl-CoA, two acyl-chains, and choline (or other headgroup) that directly participate in each GPL biosynthesis. In the experiments reported here, the two acyl chains were not distinguished though independent analysis by tandem mass spectrometry showed that the fatty acids of the major GPL examined were C16:0 and C18:1.

When cells are grown on a medium containing [U-^{13}C]-glucose each intracellular metabolite can be considered as a mixture of ^{13}C-labeled and non-labeled species. However, the fraction of ^{13}C-labeled GPL precursors, namely glycerol-3-phosphate, fatty acids and acetyl CoA that are synthesized directly from the labeled glucose is *a priori* unknown. The NMR data showed that the glycerol moiety was either natural abundance ^{13}C or $^{13}C3$. To a first approximation the acetate is considered to be present either at natural abundance or $^{13}C2$ (i.e. exclusively from glucose). Fatty acid chains are either pre-existing at natural abundance, or are synthesized *de novo* from acetyl CoA. Here we have determined isotopologue and isotopomer distributions of newly synthesized fatty acids assuming a stochastic addition from a common pool of labeled

and unlabeled acetate. Distributions at natural abundance were calculated according to the binomial theorem as:

$$p(m)=(1-f)^{n}f^{m}n!/[\,m!(n-m)!] \tag{1}$$

Where p(m) is the probability of finding m ^{13}C atoms, n is the total number of carbon atoms and f is the fraction of ^{13}C (=1.108 % at natural abundance). For the natural abundance distribution in PC34:1, n=42. For the fatty acyl moieties, the distribution was calculated as n=8 and n=9 acetyl CoA units (assuming incorporation of two carbon units per cycle to make a total of 16+18 = 34 carbons). Other isotopes are at sufficiently low abundance as to be negligible, but are distinguishable at this mass resolution.

Once ^{13}C is incorporated into the molecule, the calculation of the contributions from natural abundance becomes more complex [48–52], and the effects depend on the actual degree of label present at each position. Here we have implemented an iterative stripping approach to account for the change in the natural abundance profile on incorporation of ^{13}C atoms.

This is based on eventually decaying binomial terms (Eq. 2) that describe the multiple possible combinations of ^{13}C natural abundance incorporation for a particular molecule,

$$B(n,k)=\begin{pmatrix} C_{Max}-n \\ k-n \end{pmatrix} NA_{^{13}C}^{k-n}(1-NA_{^{13}C})^{C_{Max}-k};Bsum(n)=\sum_{k=n+1}^{C_{Max}} B(n,k) \tag{2}$$

where Cmax is the number of carbon atoms in the molecule and NA (0.01109) is the fractional natural abundance for ^{13}C. In the presence of ^{13}C enrichment, the effects of the natural abundance can be calculated using a series of decaying binomial terms as described by Eq. (3) representing the contributions from ^{13}C natural abundance for each mass isotopologue.

$$I_{M+i}=\frac{I_{M+i,NA}-\sum_{x=0}^{x<i} I_{M+x}B(x,i)}{1-Bsum(i)} \tag{3}$$

starting with i=0. I is the intensity of the ith species, with B(x,i) defined in Eq. (2)

The details of the algorithm will be presented elsewhere.

As the cells are dividing, it is expected and observed (see below) that the fraction of pre-existing GPL (natural abundance) decreases with time. Thus the following species are assumed to be present:

- **i.** m_0: natural abundance (pre-existing) GPL
- **ii.** m_0+3: unlabeled FA + labeled glycerol
- **iii.** m_0+2n: ^{13}C-labeled FA (new synthesis) + unlabeled glycerol
- **iv.** m_0+3+2n: ^{13}C-labeled FA + ^{13}C-labeled glycerol

The observed intensity distribution (I) then is a linear combination of these species, $I(n) = p_1I(m_0) + p_2I(m_0+3) + p_3I(m_0+2n) + p_4I(m_0+3+2n)$ (2) and $\Sigma p_i=1$

This implies that four parameters (three independent ones) are needed to describe the fractions of the components that can be labeled. An additional parameter, the fraction of the total acetyl CoA pool that is ^{13}C-2, is needed to describe the distribution of ^{13}C-2 units in the fatty acyl chains requires, as determined by Eq. (1).

Fatty acyl distributions were calculated using Eq. (1) as a function of the ^{13}C-2 fraction of the acetyl CoA pool. Estimates of p_i were determined as described in the results section. Non-linear regression data fitting and statistical analyses were carried out using Kaleidagraph (Synergy Software, Reading, PA).

3. Results and Discussion

We have used both high resolution NMR and FT-ICR-MS to assign GPLs, and determine their fractional enrichment in ^{13}C from the source molecule [U-^{13}C]-glucose. These data were in turn used for modeling the fractional distributions of isotopologues in the example GPL.

3.1 NMR analysis of LCC2 extracts

1D NMR showed that the major GPL species present are phosphatidylcholines, with on average two double bonds per glycerol moiety as assessed by the relative areas of the resonances at 5.35 ppm (double bond) and 5.25 ppm (glycerol C2H) (Figure 2A, C). The relative intensity of the choline methyl resonance in the 1D HSQC and 1D proton NMR spectra (Figure 1), showed that the choline head groups were not ^{13}C labeled, as expected in mammalian cells [53, 54]. In contrast, fatty acyl chains and the glycerol moieties were extensively labeled after 24 h exposure of the cells to [U-^{13}C]-glucose. By integrating the cross peak clusters in 2D TOCSY spectra of the GPLs extracted after 24 h labeling with [U-^{13}C]-glucose (cf Fig. 2B), the ^{13}C enrichment at selected atoms was determined, as previously described [38, 40]. For the glycerol moiety of the PC, we estimated the ^{13}C fraction as 44 ±1.2% U-^{13}C (and thus 56 ±1% unlabeled glycerol). Thus, in the 24 h period, nearly 50% of the GPL has been newly synthesized. This is close to that estimated by mass spectrometry, and is the main means by which the GPL have three ^{13}C atoms (see below). The fatty acyl chains in the TOCSY spectra also showed extensive ^{13}C labeling. Although the bulk CH_2 resonances of the acyl chains are largely degenerate, separate signals can be resolved from the w-methyl and the C2, C3, C4 position of the fatty acids, as well as the unsaturated carbons (albeit precise the position is not determined in these spectra). The specific patterns of labeling at C2, C3 and C4 of the fatty acids, which represent newly synthesized chains, are consistent with stochastic labeling from a pool of ^{13}C2 plus ^{12}C2 acetate (see Figure A2, Supplementary Materials), with an average ^{13}C incorporation of 46±4%.

3.2 Mass and Intensity accuracy in FT-ICR-MS

As expected, the mass accuracy and resolution of actual GPL spectra always exceeded the tune and calibration specifications for the Thermo LTQ-FT instrument. Currently, the analysis of the mass isotopologue requires that the intensities of the isotope peaks are both accurate and precise, and also that the precursor metabolite pool has the expected isotopologue distribution.

We have determined the mass spectrum intensity accuracy as follows. First, four authentic PC standards (see Methods) were analyzed as a mixture by direct infusion FT MS, and the intensity of the first four ^{13}C isotopologues were measured repeatedly. The intensities were normalized to the total out to m_0+3 and were compared for repeatability and accuracy for each of the four standards. The repeatability in terms of the coefficient of variation was 0.33% for the m_0 peak, to 1.8% for m_0+2. The accuracy was assessed by comparing the observed fractions with those calculated for a natural abundance of 1.107% ^{13}C, using Eq. (1). The rms error to m_0+3 was 0.0097±0.004, i.e. an average error of about 1%.

Second, the same procedure was carried out on control LCC2 samples at 0 h treatment (natural abundance, cf. Figure 3). For this sample the ^{13}C isotopologue distribution can be predicted according to Eq. (1), with n=42. Significant intensity was observed to m_0+3, which corresponds to 0.6% of the total. The rms error between the observed intensities and the calculated natural abundance values was 0.0039, and indicates that the analytical accuracy is of the order 0.4 %. The error increases as the intensity decreases, as expected. In practice, this implies that the useful dynamic range of the intensity ratios under these routine conditions of sensitivity is of the order 100:1, with the largest peak being typically 10 pmole/μL and eight minutes of acquisition at approximately 350 nL/min. We note that this capability is enabled by the high resolution of the FT-ICR, as each peak almost always free of intensity distortion due to ions at very close m/z, e.g. isotopomers due to other natural abundance elements such as ^{2}H, ^{15}N, and ^{18}O, as well as other structures and their isotopologues.

3.3 FT-ICR-MS analysis of LCC2 extracts

Although the NMR spectra provided positional isotope distributions, the individual GPL species were not resolved. Therefore only the enrichments of ensemble averages over all significant PC species present in the mixture were determined. In contrast, high-resolution FT-ICR-MS resolved individual GPL species and their ^{13}C isotopologues, but not the positional isotopomers.

As with GPL standards, the mass accuracy and resolution of the FT-ICR-MS for crude extracts always exceeded tune and calibration specifications. Figure 3A shows a portion of a high resolution mass spectrum of the methanolic GPL extract of LCC2 cells grown in the presence of [U-^{13}C]- glucose for 24 h. This mass range includes exact masses that correspond to PC (34:1). The m_0 peak is at m/z=760.5860; the remaining peaks belong to the ^{13}C isotopologues of the GPL, as tabulated in Table A1 (Supporting Information). The intensity of each isotopologue was normalized to the total of the isotopologues, for each time point. The resulting fractions are plotted in Fig. 3B. At t=0 the spectrum of PC(34:1) corresponds to the natural abundance carbon (and see above), but as the incubation time increased, peaks at m_0+3 and a wide distribution of m_0+2n (even mass) and m_0+3+2n (odd mass) isotopologue peaks appeared. Clearly, with increasing time, the fraction of the m_0 isotopologue decreased, whereas the m_0+3 fraction and the distribution of m_0+2n + m_0+3+2n isotopologue increased indicating de novo incorporation of ^{13}C from glucose. The odd number isotopologues (m_0+3 and m_0+3 +2n) correspond to the condensation of $^{13}C3$ glycerol with unlabeled and labeled fatty acids (FA) whereas the even number isotopologue represent PC synthesis from that of unlabeled glycerol with ^{13}C-labeled FA. Similar results were observed with other GPL species (cf Fig. A1, Supplementary Materials).

The intensity of the peaks at n=10–20 increased with time, but shifted only slightly to higher mass from 6 to 24 h. If the FA chains were being synthesized exclusively from $^{13}C2$ acetyl CoA, not only would the intensity increase, but also the mass number as eventually all new chains would approach 100% ^{13}C (cf. Supplementary Materials). As this is clearly not the case, there must be a source of $^{12}C2$ acetate persisting to 24 h. Indeed, the maxima in the distribution at 24 h are found at n=15,17 and 19. This corresponds to 12–16 ^{13}C atoms, out of a total of 34, and thus the incorporation of ^{13}C from acetyl CoA should be ca. 30–50% at 24 h.

As the degree of labeling in the glycerol moiety according to NMR was 44% (see above), these mass peaks are expected to be roughly equal in intensity. After accounting for the natural abundance intensity, and using the relations given in the Methods, we calculate that at 24 h, 35±2% of the GPL is unlabeled, 11±1% is labeled only in the glycerol moiety (m_0+3), 35% is labeled in the glycerol moiety and in the fatty acids, and the remainder (ca. 19%) is labeled in the fatty acids but not the glycerol. This makes the fraction of the glycerol labeled equal to

46%, close to the NMR estimate (see above). Similarly, the fatty acyl moieties are labeled to approx. 44%

This is shown more clearly in Figure 3C, where the fractional intensities of these four groups, corrected for natural abundance, are plotted as a function of labeling time. The fractional intensity of the m_0 peak decreased with a lag. During this time, the cells are dividing (doubling time < 24 h) so this represents in part a fractional decrease of the pre-existing GPLs as new GPLs are synthesized to make new membranes. The peak at m_0+3 represents PC in which the glycerol moiety is labeled at all three carbons, as shown conclusively by the NMR (see above), and in which the fatty acyl moieties are unlabeled. This peak approaches a steady state value of about 11 % within 6 h with a half time of 3.6 h, indicating that *de novo* biosynthesis of GPL did occur during this period, but utilized either pre-existing stores of unlabeled fatty acids (from for example internal triglyceride stores) or fatty acid biosynthesis occurred from a pool of unlabeled acetyl CoA replenished by sources other than glucose. However, as shown below, the acetyl CoA pool approach 35% ^{13}C2. As the probability of synthesizing PC(34:1) from a natural abundance ^{13}C acetyl CoA pool is extremely low, on the order of 4×10^{-7} compared with the observed 11% after 24 h, this implies that this pool is associated with recycling of intact fatty acids, not from fatty acid synthesis.

The fractions of the GPLs containing either labeled glycerol +labeled FA, and unlabeled glycerol + labeled FA were calculated by summing the natural abundance –corrected intensity of all of the even mass numbers ($n\geq2$) and all of the odd mass numbers ($n\geq5$), respectively. As shown in Fig. 2C, these fractions increased with a lag time comparable to that observed for the m_0 peak, and eventually approaching a steady state fraction of 34% for the odd number peaks and 20% for the even number peaks.

3.4 Model Simulations

The NMR and FT-ICR-MS data support a minimal model for the GPL ^{13}C-isotope profile as outlined in Figure 4. [U-^{13}C]-glucose, the sole source of ^{13}C in these experiments, generates both labeled glycerol-3-phosphate and acetyl CoA. Unlabeled glycerol phosphate is also produced in part by turnover of GPL and internal triglyceride stores, which also generate free fatty acids that can be reincorporated into GPL or be oxidized to unlabeled acetyl CoA. Both unlabeled and labeled glycerol moieties are incorporated into GPLs stochastically, as is the case for acetyl CoA, as shown by the NMR data. Model calculations showed that the fraction of unlabeled GPL decreased from 100% at time 0 to 35% at 24 h. The fraction of GPL with ^{13}C3-glcyerol and unlabeled acyl chains increased to 11% at 24 h while those of GPL with unlabeled glycerol + ^{13}C-labeled acyl chains or ^{13}C-labeled glycerol+^{13}C-labeled acyl chains reached 20% and 35%, respectively (cf. Fig. 3C and Supplementary Materials). The sum of all fractions for a given time point is close to 1.

The best determined parameters are p_1 and p_2, which are limited primarily by the analytical errors of the intensity ratio determinations (i.e. of the order 0.5–1% for these intense peaks, see above). Other errors include spectral overlap and relatively low intensity of mass peaks. Overall, the errors appear to be less than 5–10%, and the parameter estimates are in good agreement with independent NMR data for the labeling of the glycerol backbone (see above).

The remaining unknown is the distribution of ^{13}C in the fatty acyl chains. As described above, the simplest possible model is one in which there is a single pool of acetyl CoA that approaches isotopic steady state at sufficiently long times, and that acetyl CoA units are stochastically incorporated into the newly synthesized acyl chains. The expected distributions in the acetyl CoA pool and in the GPLs are given in the Supplementary Materials. Simulations using Eq. (1) as a function of the fraction of ^{13}C2-acetyl CoA indicated that this pool be of the order 35–40% of the total at 24 h, in agreement with the rough estimate obtained from the position of

the maximum (Fig. 3A). Using this, and the values of p_1-p_4 given in Appendix 1, we have simulated the distribution of PC(34:1) using stochastic incorporation of C16 and C18 chains. This is compared with the observed distribution in Figure 5.

The general shape of the calculated distribution agrees with the experimental fractions, though there are some quantitative disagreements that reflect in part the measurement errors as discussed above, and deficiencies in the simple model. For example, it was assumed that the acetyl CoA units showed no scrambling (i.e. the ^{13}C1 acetates are at natural abundance), and that the synthesis was strictly stochastic The former condition was not fully met, according to the NMR data, which indicated the presence of ^{13}C1 acetyl units at the 5% level.

A more detailed model and biological interpretation will be presented elsewhere.

4. Conclusions

We have shown that FT-ICR-MS, even under short acquisitions of <9 min of low pmol/μL concentrations of GPLs, provides sufficient resolution and high quality intensity data for determining ^{13}C isotopologue distributions of individual GPL species in complex mixtures, that result from [U-^{13}C]-glucose as a precursor. This produces m_0+3 glycerol and m_0+2 acetate, which are therefore distinguishable in the mass isotopologue distributions.

When combined with positional isotope labeling information from high resolution NMR data, it is possible to determine the fractions of the contributing pools of the metabolites used in the synthesis of the particular GPL species. The key facets of the FT-ICR-MS is the combination of direct infusion with very high mass resolution which eliminates contamination from similar m/z ions, very high mass accuracy for rapid assignments, and intensities that exhibit high accuracy and precision of the isotopologue abundances.

Time course modeling of the fractional distribution of selected isotopologues of PC(34:1) revealed a lag in the incorporation of acyl chains newly synthesized from glucose while the synthesis of the glycerol moiety from glucose occurred without delay and reached a steady state in 6 h (cf Figure 3C). The model analysis also indicated the presence of unlabeled glycerol and acetyl CoA pools (possibly derived from pre-existing GPL stores) up to 24 h of labeling time. Moreover, the incorporation of labeled and unlabeled glycerol and acetyl CoA into PC16,18 was essentially stochastic. These data therefore provide a basis for analyzing the synthesis of GPL using glucose carbon, as well as providing information about turnover of GPLs under conditions of net growth.

We have illustrated the principles for a particular glycerophosphatidylcholine in positive ion mode. Clearly this is applicable to any PC, but also, by extension to other GPL in either positive or negative ion mode, including PE and PS and sphingolipids, with the proviso that additional analysis would be needed if their headgroups were also metabolically labeled. PC(34:1) is the most abundant GPL in these samples. However, comparable isotope distributions were observed for other GPL species of different chain lengths in these samples (Fig. A1, Supplementary Materials), and indeed in other breast cell lines (A.N. Lane, T. W-M. Fan and R.M. Higashi, unpublished data).

The same approach can also be readily applied to study the synthesis and turnover of other important metabolites such as nucleotides using labeled glucose or other labeled precursors.

Supplementary Material

Refer to Web version on PubMed Central for supplementary material.

Acknowledgments

This work was supported in part by National Science Foundation EPSCoR grant # EPS-0447479, NIH Grant Number P20RR018733 from the National Center for Research Resources, 1R01CA118434-01A2 from the National Cancer Institute, the Kentucky Challenge for Excellence, Susan G. Komen Foundation BCTR0503648, and the Brown Foundation.

Abbreviations

BHT
butylated hydroxytoluene

DMPC
dimyristoylphosphatidylcholine

DPPC
dipalmitoylphosphatidylcholine

DSPC
distearoylphosphatidylcholine

DOPC
dioleoylphosphatidylcholine

GPL
glycerophospholipid

PC
phosphatidylcholine

References

1. Metzler, DE. Biochemistry. Academic Press; Sa Diego: 2001.
2. Furuta E, Pai SK, Zhan R, Bandyopadhyay S, Watabe M, Mo YY, Hirota S, Hosobe S, Tsukada T, Miura K, Kamada S, Saito K, Iiizumi M, Liu W, Ericsson J, Watabe K. Cancer Research 2008;68:1003–1011. [PubMed: 18281474]
3. Orita H, Coulter J, Lemmon C, Tully E, Vadlamudi A, Medghalchi SM, Kuhajda FP, Gabrielson E. Clinical Cancer Research 2007;13:7139–7145. [PubMed: 18056164]
4. Swinnen JV, Brusselmans K, Verhoeven G. Current Opinion in Clinical Nutrition and Metabolic Care 2006;9:358–365. [PubMed: 16778563]
5. Piyathilake CJ, Frost AR, Manne U, Bell WC, Weiss H, Heimburger DC, Grizzle WE. Human Pathology 2000;31:1068–1073. [PubMed: 11014573]
6. Cunnane SC. Progress in Lipid Research 2003;42:544–568. [PubMed: 14559071]
7. German JB, Gillies LA, Smilowitz JT, Zivkovic AM, Watkins SM. Current Opinion in Lipidology 2007;18:66–71. [PubMed: 17218835]
8. Wiest MM, Watkins SM. Current Opinion in Lipidology 2007;18:181–186. [PubMed: 17353667]
9. Hunt AN, Postle AD. Methods 2006;39:104–111. [PubMed: 16831558]
10. Wakelam MJO, Pettitt TR, Postle AD. Lipidomics and Bioactive Lipids: Mass-Spectrometry-Based Lipid Analysis 2007;432:233–246.
11. Postle AD, Wilton DC, Hunt AN, Attard GS. Progress in Lipid Research 2007;46:200–224. [PubMed: 17540449]
12. Carrasco MP, Jimenez-Lopez JM, Segovia JL, Marco C. Comparative Biochemistry and Physiology B-Biochemistry & Molecular Biology 2002;131:491–497.
13. Bleijerveld OB, Houweling M, Thomas MJ, Cui Z. Analytical Biochemistry 2006;352:1–14. [PubMed: 16564484]

14. Bulotta A, Perfetti R, Hui HX, Boros LG. Journal of Lipid Research 2003;44:1559–1565. [PubMed: 12777469]
15. Boros LG, Cascante M, Lee WNP. Drug Discovery Today 2002;7:364–372. [PubMed: 11893545]
16. Neese RA, Siler SQ, Cesar D, Antelo F, Lee D, Misell L, Patel K, Tehrani S, Shah P, Hellerstein MK. Analytical Biochemistry 2001;298:189–195. [PubMed: 11700973]
17. Di Buono M, Jones PJH, Beaumier L, Wykes LJ. Journal of Lipid Research 2000;41:1516–1523. [PubMed: 10974059]
18. Siler SQ, Neese RA, Hellerstein MK. American Journal of Clinical Nutrition 1999;70:928–936. [PubMed: 10539756]
19. LligonaTrulla L, Arduini A, Aldaghlas TA, Calvani M, Kelleher JK. Journal of Lipid Research 1997;38:1454–1462. [PubMed: 9254070]
20. Lee WNP, Bassilian S, Guo ZK, Schoeller D, Edmond J, Bergner EA, Byerley LO. American Journal of Physiology 1994;266:E372–E383. [PubMed: 8166257]
21. Lee WP, Bassilian S, Bergner EA, Wals P, Katz J. Clinical Research 1994;42:A28–A28.
22. Smith SB. Federation Proceedings 1983;42:815–815.
23. Smith SB. Archives of Biochemistry and Biophysics 1983;221:46–56. [PubMed: 6830264]
24. DeLong CJ, Baker PRS, Samuel M, Cui Z, Thomas MJ. Journal of Lipid Research 2001;42:1959–1968. [PubMed: 11734568]
25. Wang C, Xie SG, Yang J, Yang Q, Xu GW. Analytica Chimica Acta 2004;525:1–10.
26. Barroso B, Bischoff R. Journal of Chromatography B-Analytical Technologies in the Biomedical and Life Sciences 2005;814:21–28.
27. Peterson BL, Cummings BS. Biomedical Chromatography 2006;20:227–243. [PubMed: 16138296]
28. Schwudke D, Hannich JT, Surendranath V, Grimard V, Moehring T, Burton L, Kurzchalia T, Shevchenko A. Analytical Chemistry 2007;79:4083–4093. [PubMed: 17474710]
29. Schwudke D, Oegema J, Burton L, Entchev E, Hannich JT, Ejsing CS, Kurzchalia T, Shevchenko A. Analytical Chemistry 2006;78:585–595. [PubMed: 16408944]
30. He H, Conrad CA, Nilsson CL, Ji YJ, Schaub TM, Marshall AG, Emmett MR. Analytical Chemistry 2007;79:8423–8430. [PubMed: 17929901]
31. Milne SB, Ivanova PT, DeCamp D, Hsueh RC, Brown HA. Journal of Lipid Research 2005;46:1796–1802. [PubMed: 15897608]
32. Byrdwell WC, Sato H, Schwarz AK, Borchman D, Yappert MC, Tang DX. Lipids 2002;37:1087–1092. [PubMed: 12558059]
33. Castro V, Dvinskikh SV, Widmalm G, Sandstrom D, Maliniak A. Biochimica Et Biophysica Acta-Biomembranes 2007;1768:2432–2437.
34. Nicholls AW, Nicholson JK, Haselden JN, Waterfield CJ. Biomarkers 2000;5:410–423.
35. Mahrous EA, Lee RB, Lee RE. Journal of Lipid Research 2008;49:455–463. [PubMed: 17982136]
36. Fan TW, Lane AN. Progress in NMR Spectroscopy 2008;52:69–117.
37. Lane AN, Fan TW-M, Higashi RM. IUBMB Life 2008;60:124–129. [PubMed: 18380001]
38. Lane, AN.; Fan, TW.; Higashi, RM. Isotopomer-based metabolomic analysis by NMR and mass spectrometry. In: John, HWD.; Correia, J., editors. Biophysical Tools for Biologists. Vol. 1. Academic Press; San Diego: 2008. p. 541-588.
39. Fan TW-M, Kucia M, Jankowski K, Higashi RM, Rataczjak MZ, Rataczjak J, Lane AN. Molecular Cancer 2008;7:79. [PubMed: 18939998]
40. Lane AN, Fan TW. Metabolomics 2007;3:79–86.
41. Fan TWM, Higashi RM, Lane AN. Drug Metabolism Reviews 2006;38:707–732. [PubMed: 17145697]
42. Fan T, Bandura L, Higashi R, Lane A. Metabolomics 2005;1:1–15.
43. Fan TWM, Lane AN, Higashi RM. Current Opinion in Molecular Therapeutics 2004;6:584–592. [PubMed: 15663322]
44. Fan TWM, Lane AN, Higashi RM. Russian Journal of Plant Physiology 2003;50:787–793.

45. Lane, AN.; Fan, TW.; Higashi, RM. Isotopomer-based metabolomic analysis by NMR and mass spectrometry. In: John, HWD.; Correia, J., editors. Biophysical Tools for Biologists. Vol. 1. Academic Press; San Diego: 2007. p. 541-588.

46. Tang Y, Pingitore F, Mukhopadhyay A, Phan R, Hazen TC, Keasling JD. Journal of Bacteriology 2007;189:940–949. [PubMed: 17114264]

47. Pingitore F, Tang YJ, Kruppa GH, Keasling JD. Analytical Chemistry 2007;79:2483–2490. [PubMed: 17305312]

48. Zhang X, Hines W, Adamec J, Asara JM, Naylor S, Regnier FE. Journal of the American Society for Mass Spectrometry 2005;16:1181–1191. [PubMed: 15922621]

49. van Winden WA, Wittmann C, Heinzle E, Heijnen JJ. Biotechnology and Bioengineering 2002;80:477–479. [PubMed: 12325156]

50. Wahl SA, Dauner M, Wiechert W. Biotechnology and Bioengineering 2004;85:259–268. [PubMed: 14748080]

51. Mashego MR, Wu L, Van Dam JC, Ras C, Vinke JL, Van Winden WA, Van Gulik WM, Heijnen JJ. Biotechnology and Bioengineering 2004;85:620–628. [PubMed: 14966803]

52. Snider RK. Journal of the American Society for Mass Spectrometry 2007;18:1511–1515. [PubMed: 17583532]

53. Zeisel SH. Nutrition 2000;16:669–571. [PubMed: 10906592]

54. Glunde K, Jie C, Bhujwalla ZM. Cancer Research 2004;64:4270–4276. [PubMed: 15205341]

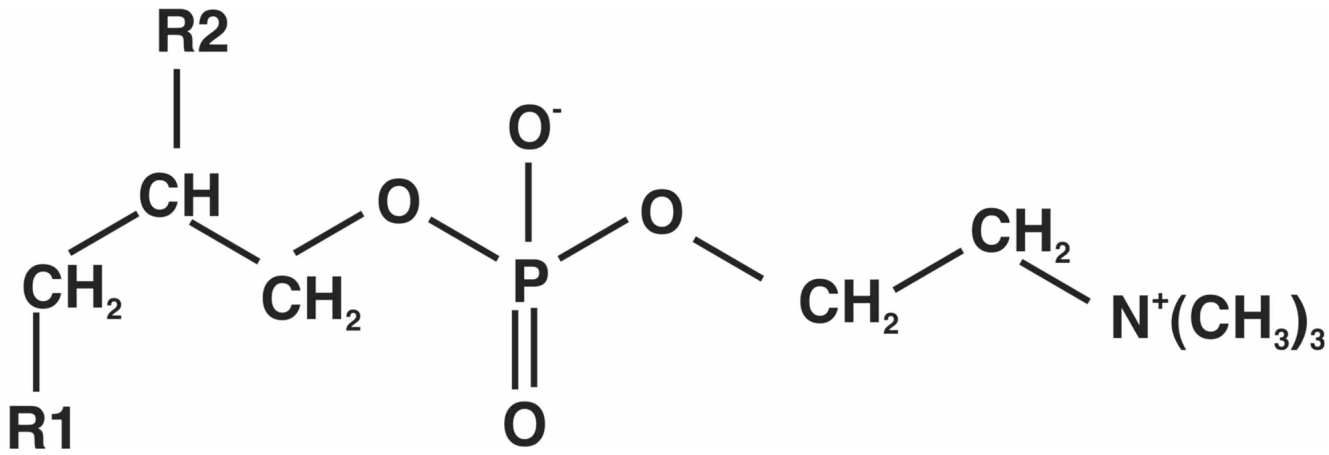

Figure 1.
Structure of a glycerophosphatidyl choline

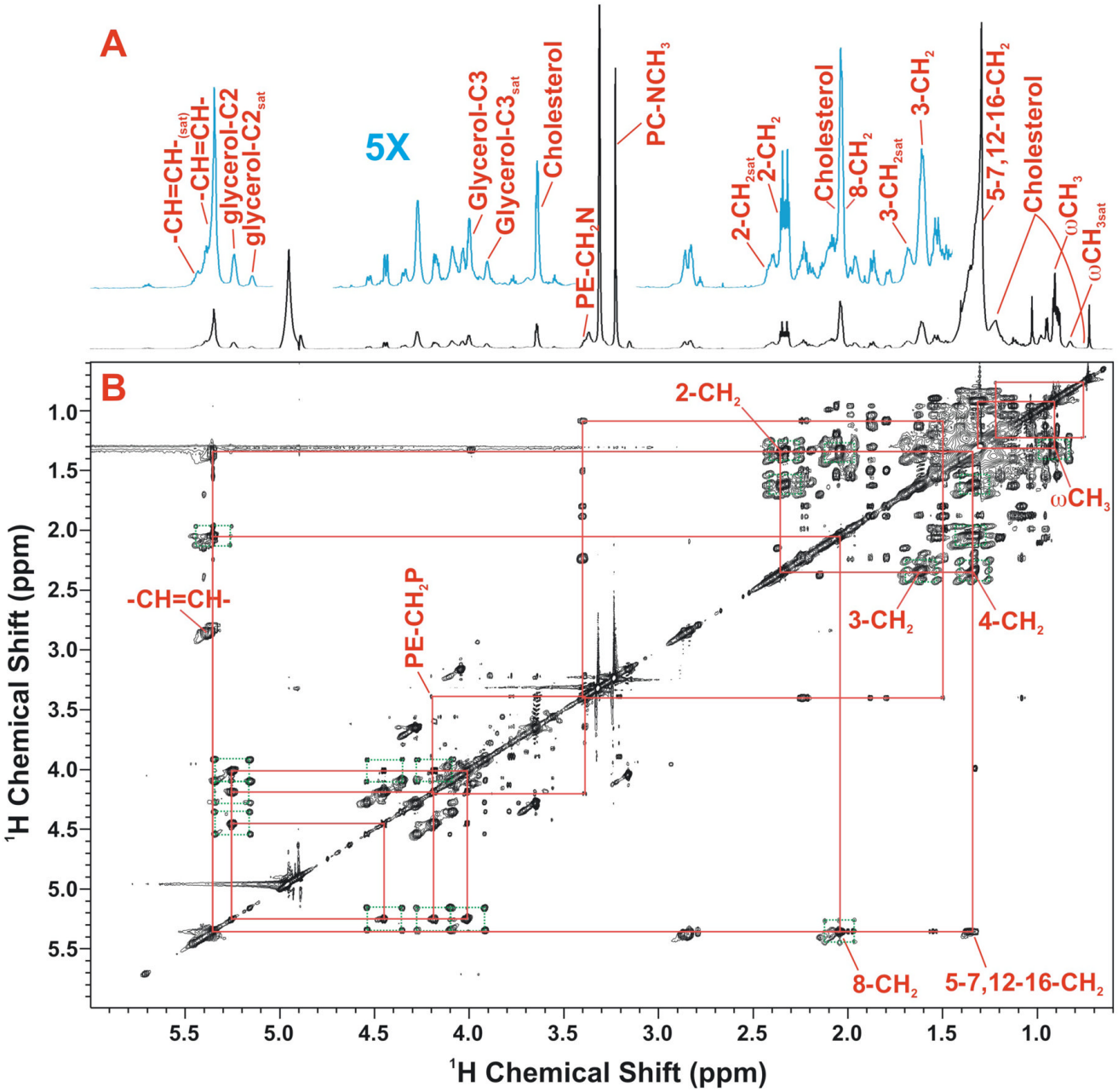

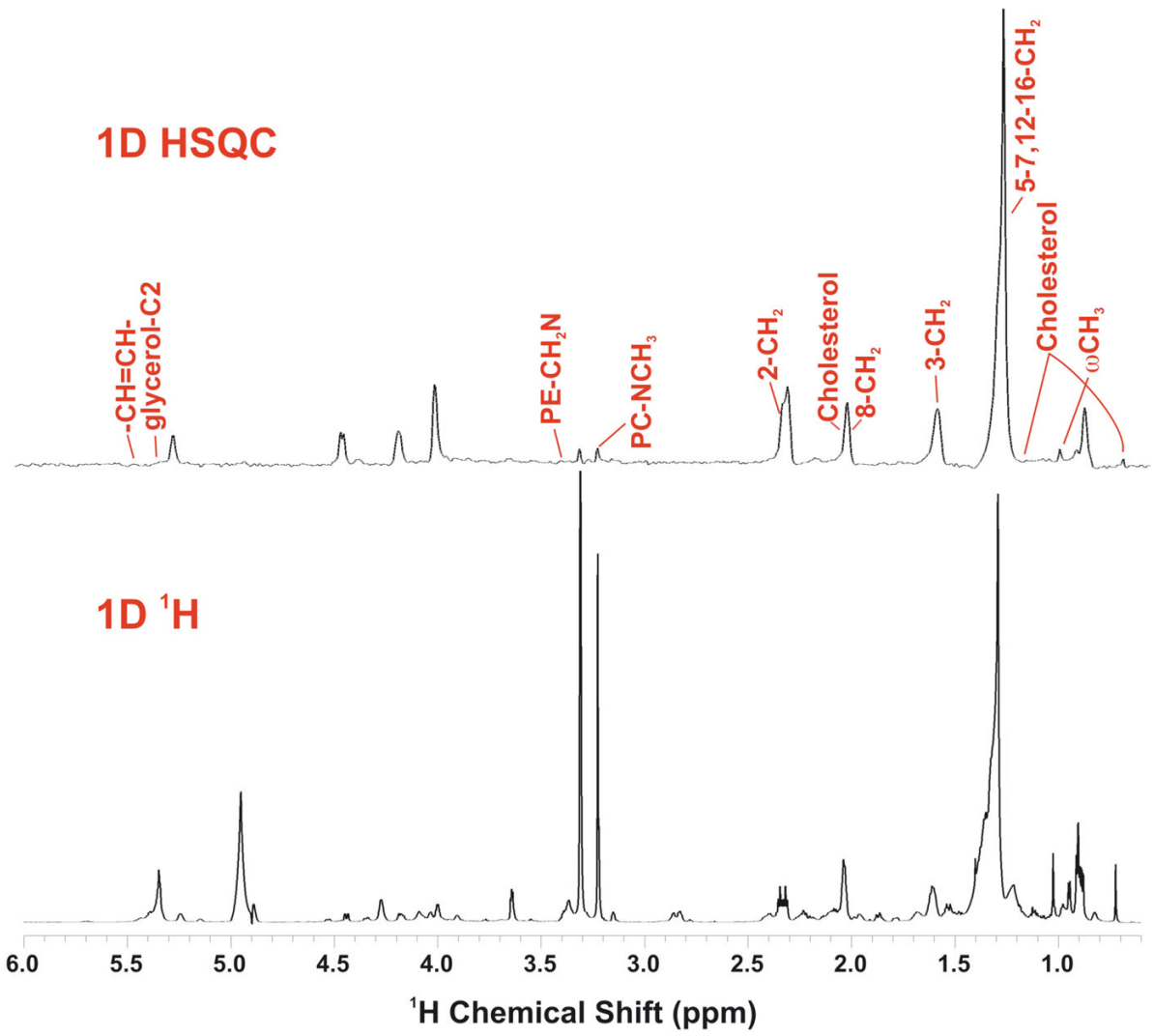

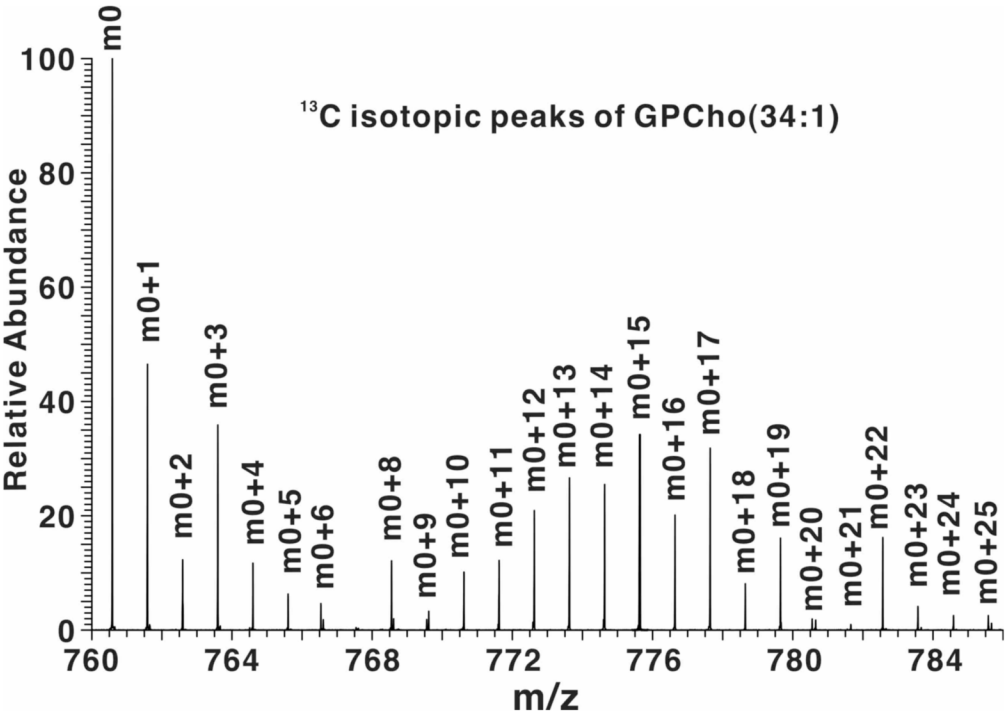

Figure 2. High resolution NMR spectra of a methanolic extract of LCC2 cells

Glycerophospholipids were extracted from LCC2 cells grown in the presence of 10 mM [U-^{13}C]- glucose for 24 h as described in the text. NMR spectra were recorded at 800 MHz, 20°C as described in the methods.

A,B. TOCSY spectrum recorded with a mixing time of 50 ms with 1D 1H NMR spectrum. The TOCSY spectrum was recorded at 18.8 T 293 K with 50 ms mixing time at a B_1 field strength of 9 kHz. The data were processed with one linear prediction and zerofilling in t_1 and apodized using an unshifted Gaussian function in both dimensions.

C. 1D NMR spectra

Top: 1D ^{13}C-edited ^{1}H (HSQC) spectrum

Bottom: high resolution ^{1}H NMR spectrum

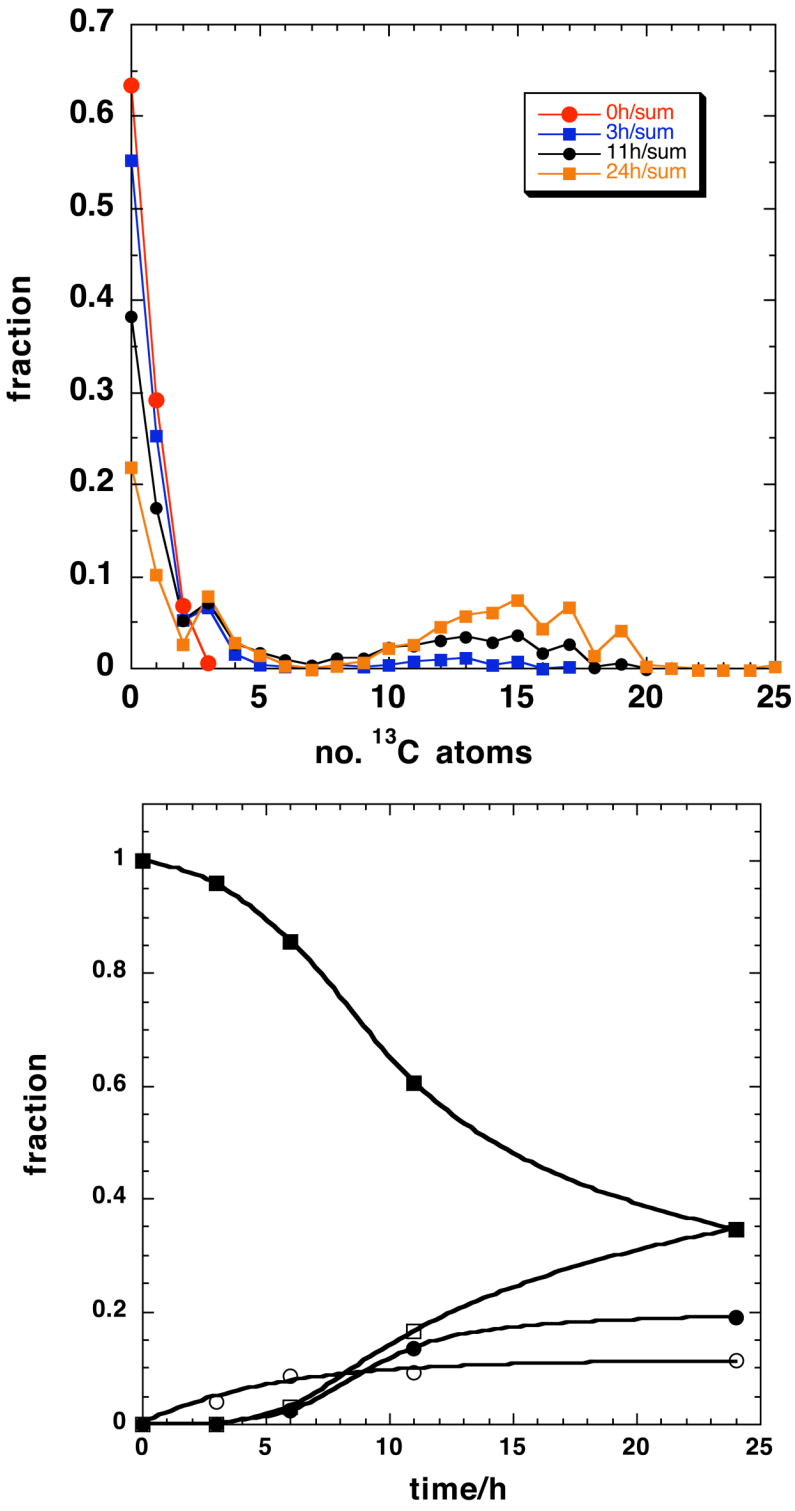

Figure 3. High-resolution FT-ICR mass spectrum of a methanolic extract of LCC2 cells

A. FT-ICR-MS profile spectrum of an LCC2 methanol extract after 24 h labeling with [U-^{13}C]-glucose. A close up of the m/z region from 760 to 782 is shown. The accurate masses (better than 1 ppm) at high resolution (>100,000 at measured mass) enable assignment of the

GPLs and their isotopologues. Masses externally calibrated, and secondarily calibrated with respect to internal standard reserpine and intensities have been arbitrarily scaled to 100 units for m_0 at m/z=760.5860.

B. Mass distribution of PC 34:1 normalized to the total intensity as a function of time. The distribution at 0 h is indistinguishable from the expected natural abundance intensity. Line graphs are used here for clarity only; there are no values implied in between the data points

C. Time courses of selected mass peaks. ■ m_0, □ m_0+3, ● $\Sigma(m_0+2n)$; ❍ $\Sigma(m_0+3+2n)$. The m_0+3 intensities were fitted to $a(1-\exp(-kt))$ with a= 0.11±0.008 and k=0.19 ±0.04 h^{-1}

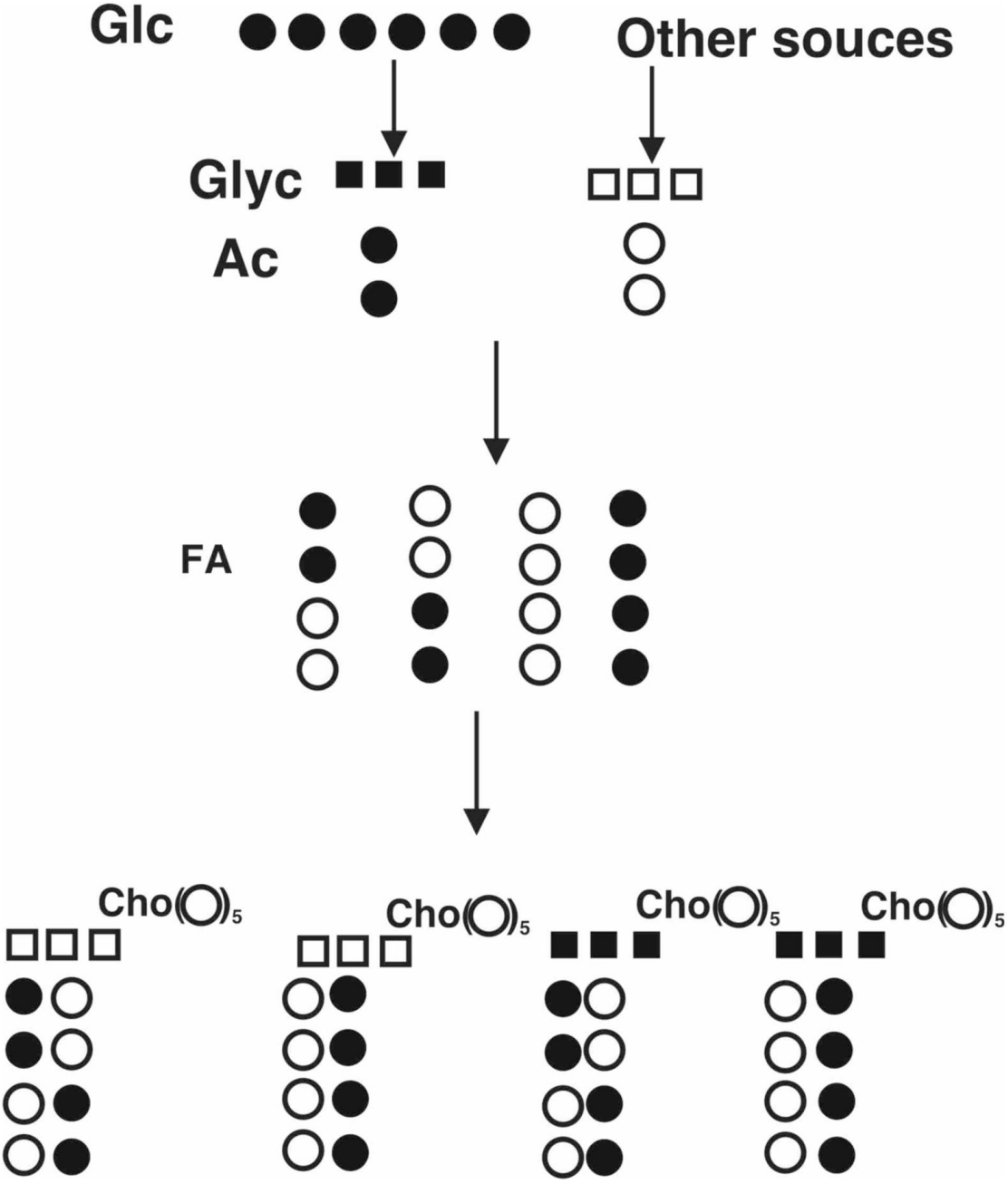

Figure 4. Glycerophosphatidylcholine biosynthesis model

Only carbons atoms that can become biosynthetically labeled from glucose are shown (the choline headgroup is unlabeled, see text). Glc = glucose, Glyc = glycerol.

Filled circles represent ^{13}C and open circles ^{12}C. Glycerol and acetyl carbons derive from [U-^{13}C]-glucose or from unlabeled sources. Fatty acids are built up from labeled and unlabeled Acetyl CoA, stochastically. For butanoate (shown) there are 4 possible isotopomers. These can condense with either unlabeled (natural ^{13}C abundance) glycerol, or labeled glycerol. From 4 fatty acyl isotopomers, condensation with each glycerol moiety generates 16 possible diacyl GPL molecules, for which there are two ways of getting both chains unlabeled, two ways of both chains fully labeled (8 ^{13}C), two ways of having two ^{13}C, and four of having 4 ^{13}C. These

possibilities equally exist for both forms of glycerol, leading to two peaks comprising m_0, m_0+2, m_0+4, m_0+8 and m_0+3, m_0+5, m_0+7 and m_0+11. Some fraction of the total will also correspond to pre-existing GPL that has not been turned over (i.e. only natural abundance ^{13}C). Only four representative dibutyl GPL isotopologues (out of 32) are shown.

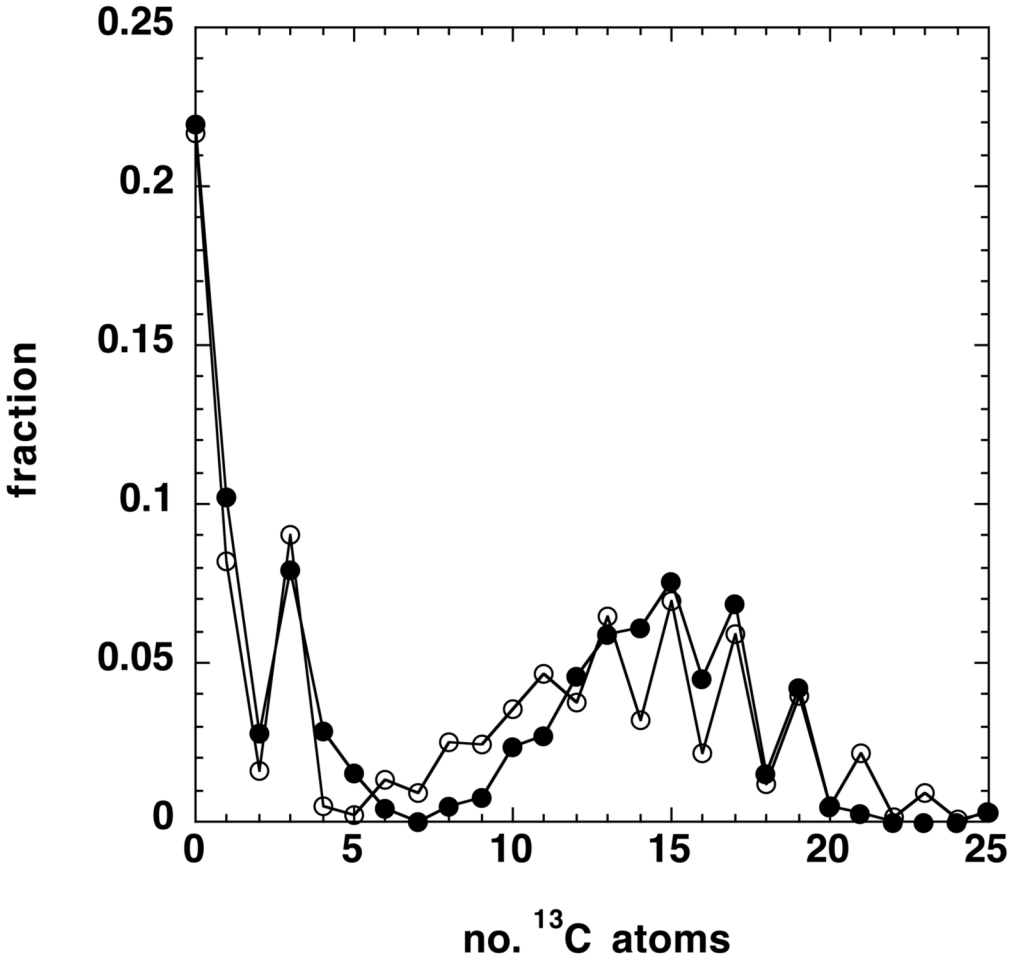

Figure 5.

Simulated isotopologue **distribution at 24h**

The isotopologue distribution at 24 h post ^{13}C glucose labeling was calculated using Eq. (2) and the appropriate values of p given in the text. The isotopologues of the fatty acyl chains were calculated using Eq. 1 as described in the text, for a pool of acetyl CoA that was 35% $^{13}C2$ acetate.

(●) simulated distribution (❍) observed distribution.